PERGAMON

Journal of Atmospheric and Solar-Terrestrial Physics 63 (2001) 1447–1453

Journal of ATMOSPHERIC AND SOLAR-TERRESTRIAL PHYSICS

www.elsevier.com/locate/jastp

# Further study of the dynamics of two-dimensional MHD coherent structures — a large-scale simulation

C.C. Wu[a,*], Tom Chang[b]

[a] Department of Physics and Astronomy, University of California, Los Angeles, CA, USA

[b] Center for Space Research, Massachusetts Institute of Technology, Cambridge, MA, USA

**Abstract**

We report new large-scale two-dimensional MHD simulations regarding the random onset and interactions of localized coherent structures as well as the long-range behavior of such stochastic systems. With a magnetic shear, multiple coherent structures are formed and aligned with the imposed current sheet due to fluctuation-induced, nonlinear instabilities. These results exhibit certain aspects of the intermittent turbulence model of sporadic localized reconnections for the Earth's magnetotail recently suggested by Chang. 

*Keywords:* Magnetotail turbulence; Self organized criticality; MHD turbulence simulation

## 1. Introduction

Recently, Chang (1998a,b, 1999) proposed a dynamical model involving the generation, dispersing, and merging of multiscale coherent plasma structures to address the intermittent turbulent behavior of the Earth's magnetotail revealed by satellite observations (Angelopoulos et al., 1996, 1999; Lui, 1998). In this model, the dynamics of the magnetotail is related to the stochastic behavior of a nonlinear dynamical system near forced and/or self-organized criticality (FSOC) and the onset of substorm to an associated global fluctuation-generated, nonlinear instability due to the presence of pre-existing finite fluctuations. Accordingly, the fluctuation spectra are expected to exhibit multi-fractal behavior and the dynamics of the magnetotail behaves essentially as a low-dimensional system. This conclusion seems to agree with the results of some of the recent nonlinear dynamics calculations (Baker et al., 1990; Vassiliadis et al., 1990; Klimas et al., 1992; Sharma et al., 1993) and observations (Hoshino et al., 1994; Milovanov et al., 1996; Lui, 1998).

* Corresponding author. Tel.: +1-310-825-8103; fax: +1-310-206-3051.

*E-mail address:* wu@physics.ucla.edu (C.C. Wu).

We report here further results from large-scale MHD simulations that confirm our previously reported preliminary findings (Wu and Chang, 2000). MHD turbulence has been studied extensively, mostly through large-scale 2D and 3D computations; some of the references are Biskamp and Welter (1989), Craddock et al. (1991), Galtier et al. (1999), and Wu and Chang (2000). Current sheet formation has been observed for low mode number initial conditions. On the other hand, long-lived isolated current filaments are found to evolve from an initially random current distribution (Craddock et al., 1991). For sufficiently high Reynolds numbers, genuine small-scale turbulence can occur in 2D (Biskamp and Welter, 1989). Our emphasis here is on the interaction of the coherent structures, the resulting localized reconnection processes, and the long-range behavior of the system. It will not be the purpose of this paper to demonstrate the critical nature of the dynamic behavior. We also consider the effects of sheared magnetic field; thus, the calculations are more relevant to the dynamics of the magnetotail in the neutral sheet region. With a magnetic shear, the coherent structures are found to align with the background current sheet and a fluctuation-induced, nonlinear instability is observed. These features are consistent with the expectation of Chang's model.

1364-6826/01/$ - see front matter 
PII: S1364-6826(00)00246-7

## 2. Outline of the simulation

In our simulations, we solved compressible MHD equations on a computer as an initial and boundary value problem. The ideal compressible MHD equations are

$$\frac{\partial \rho}{\partial t} = -\nabla \cdot (\rho \mathbf{v}), \tag{1}$$

$$\frac{\partial (\rho \mathbf{v})}{\partial t} = -\nabla \cdot \left[ \rho \mathbf{v}\mathbf{v} + \mathbf{I}\left( p + \frac{B^2}{2} \right) - \mathbf{B}\mathbf{B} \right], \tag{2}$$

$$\frac{\partial \mathbf{B}}{\partial t} = \nabla \times (\mathbf{V} \times \mathbf{B}), \tag{3}$$

$$\frac{\partial \varepsilon}{\partial t} = -\nabla \cdot \left[ \left( \frac{\rho v^2}{2} + \frac{p}{\gamma - 1} + p \right) \mathbf{v} - (\mathbf{V} \times \mathbf{B}) \times \mathbf{B} \right]. \tag{4}$$

Here, the mass density, the pressure, the velocity, and the magnetic field are denoted by $\rho$, $p$, $\mathbf{v}$, and $\mathbf{B}$, respectively; $\gamma$ is the ratio of specific heats. The magnetic field satisfies the divergence-free condition and the energy density ($\varepsilon$) is given by $\varepsilon = \rho v^2/2 + B^2/2 + p/(\gamma - 1)$. Plasmas are assumed to obey perfect gas law with $\gamma = 2$.

We used a second-order accurate code (Tadmor and Wu, in preparation), which applied the central scheme developed by Nessyahu and Tadmor (1990) and Kurganov and Tadmor (1999). The code is constructed in conservative form so that the total mass, total energy, total magnetic fluxes and total momenta are conserved. Also, in order to reach the small-diffusion limit we do not include explicit diffusion terms in Eqs. (1)–(4). However, in the numerical scheme there is numerical diffusion, which concentrates at places where the gradient is high; it allows, for example, magnetic field reconnection to proceed.

The three calculations reported here were carried out with $512 \times 512$ grid points in a doubly periodic ($x$, $z$) domain of length $2\pi$ in both directions. This extends our previously reported calculations to larger system dimensions. The initial condition consists of random magnetic field, which is specified by a flux function, and velocity. The flux function and the two components of velocity are proportional to $k^2 \exp(-\alpha k^2)$ in the Fourier space, with $\alpha$ being a constant. For runs 1 and 2, $\alpha = 0.01$ and the initial kinetic energy is peaked at $k = 10$; for run 3, $\alpha = 0.0025$ and the kinetic energy is peaked at $k = 20$. The initial fluctuation levels are set so that for all three cases the maximum amplitude of the magnetic field is 0.3 and the maximum value of the velocity is 0.2. For cases 2 and 3, in addition to the fluctuations a sheared magnetic field $B_x = 0.1 \cos z$ is imposed. These values should be compared with the initial values of pressure and density, which are given by the pressure balance equation $p + B^2/2 = 0.8$ and by the uniform temperature of 1, i.e., $\rho = p$. The plasma $\beta$ is high for the runs.

## 3. Simulation results — no background magnetic field

We consider first the dynamics of 2D MHD coherent structures for a simulated homogeneous turbulent plasma without the influence of an average background magnetic field. Initially, the configuration consists of randomly distributed current filaments. We observe that filaments of the same polarity, i.e., currents flowing in the same direction, tend to attract and coalesce; and after the merging, a larger island is formed. On the other hand, current filaments of opposite polarity tend to repel each other. Our results show that the system evolves to a set of magnetic coherent structures, as shown in Fig. 1 for the results at $t = 300$ and 600. For reference, the sound wave and Alfvén wave traveling times through a distance of $2\pi$ are about 4.4 and 60, respectively. The left-hand side column of Fig. 1 shows the magnetic field lines, which are the level curves of the magnetic flux. Since the difference between adjacent levels is set by same amount of flux, the relative magnitude of the magnetic field can be inferred from these contours. A region with large changes in the flux, showing with more contour curves, indicates stronger magnetic field and a region with small changes in the flux, thus with fewer contours, means weaker magnetic field. The directions of the magnetic fields can easily be induced from the plots of the corresponding currents in the right-hand side column of Fig. 1. The field lines point in the clockwise (counter-clockwise) direction if the current density is positive (negative) in the $y$ direction. Fig. 1 shows magnetic islands of various sizes formed. At the center of each island is an isolated current filament. The structures are very persistent and one may be tempted to associate them with observed thin current sheet in the magnetotail (Sergeev et al., 1993). They are circularly symmetric and thus naturally satisfy the force-free condition of $(\mathbf{B} \cdot \boldsymbol{\nabla})J = 0$. This is clearly demonstrated for larger and isolated islands.

A standard technique to gauge the behavior of intermittent turbulence is through the spectra of turbulent fluctuations. Chang has suggested that near SOC, the correlations among the fluctuations of the random dynamic fields are extremely long-range and the fluctuation spectra have a power-law behavior. Fig. 2 is a plot of the self-correlation of $(\delta B_x)^2$, i.e., the ensemble average $\langle (\delta B_x)^2 (\delta B_x)^2 \rangle$, with respect to the separation in $x$, $\delta x$, for the results at $t = 600$; $\delta B_x = B_x - \bar{B}_x$ with $\bar{B}_x$ denoting the local average of $B_x$ over nine cells. It suggests power-law behavior up to $\delta x \sim 0.8$.

Fig. 3 shows an example of the magnetic merging process. The two islands near $(x, z) = (4.2, 0.7)$ at $t = 300$ are shown to merge into one at $t$ around 420. It is similar to the merging process caused by the coalescence instability of magnetic islands (Pritchett and Wu, 1979). The rather smooth merging process as depicted in Fig. 3 indicates that the magnetic Reynolds number from the code is small with respect to the local reconnection region. If we were to have more resolution and thus larger Reynolds number, a chain of magnetic islands of smaller sizes may form at the interface of the merging two islands.

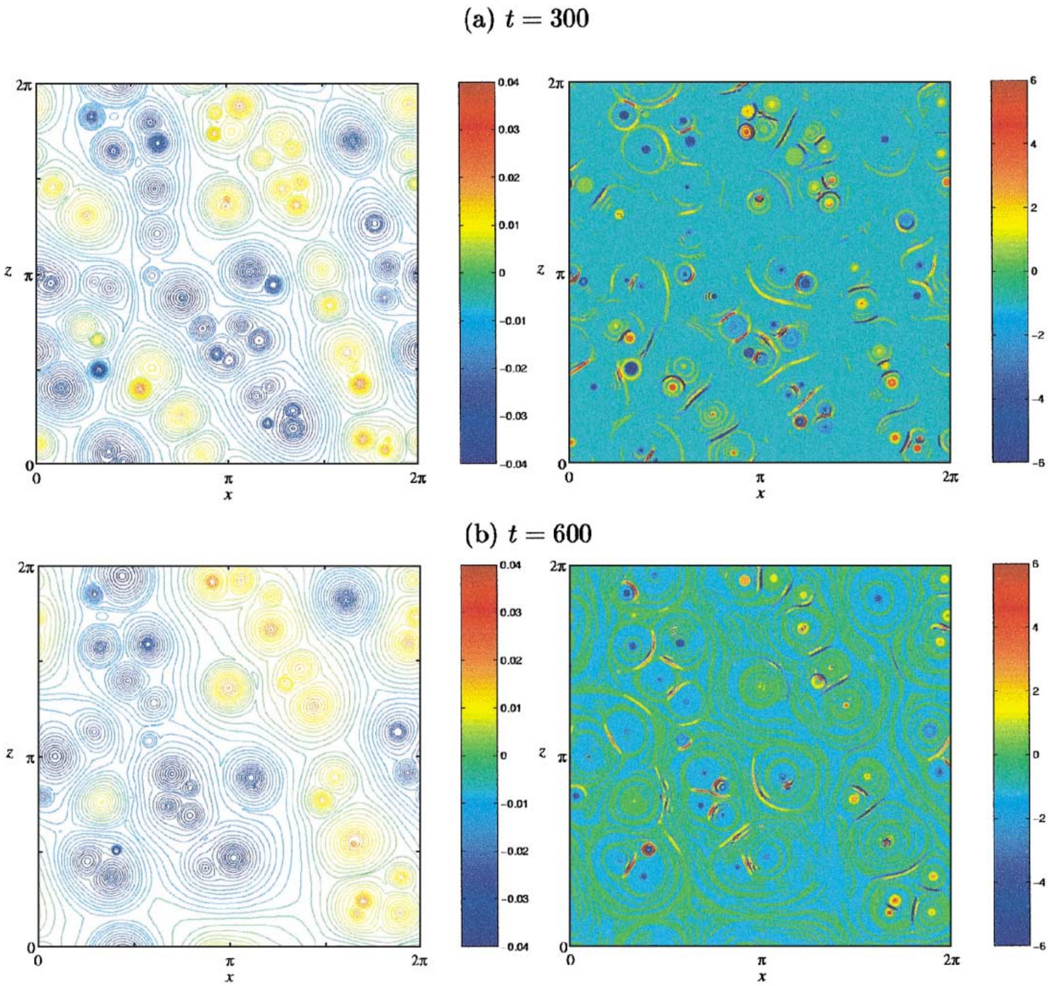


Fig. 1. Results of Case 1 at $t = 300$ and 600. The magnetic field lines (contours of the magnetic flux) are shown in the left-hand side column; the corresponding current distributions $J_y$ are shown in the right-hand side column.

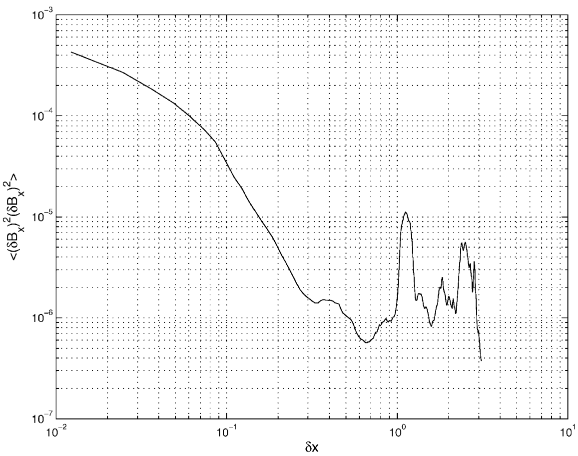


Fig. 2. Results of Case 1 at $t = 600$. The self-correlation of $(\delta B_x)^2$, indicating a power-law behavior.

We ended the simulation at $t = 600$. We expect the merging of coherent structures to continue after $t = 600$, but with a slower rate. While the calculations show the evolution of coherent structures emerging from random fluctuations, it does not exhibit the true essence of MHD turbulence. The reason is perhaps that the numerical Reynolds numbers in the calculation are not high enough so that the generation mechanism of small scale turbulence through stretching, folding, and/or tearing instability of the current sheets does not set in.

## 4. Simulation results — with a background sheared magnetic field

We now consider the influence of an average background sheared magnetic field on the dynamics of the coherent structures. The motivation here is to mimic the effect of the

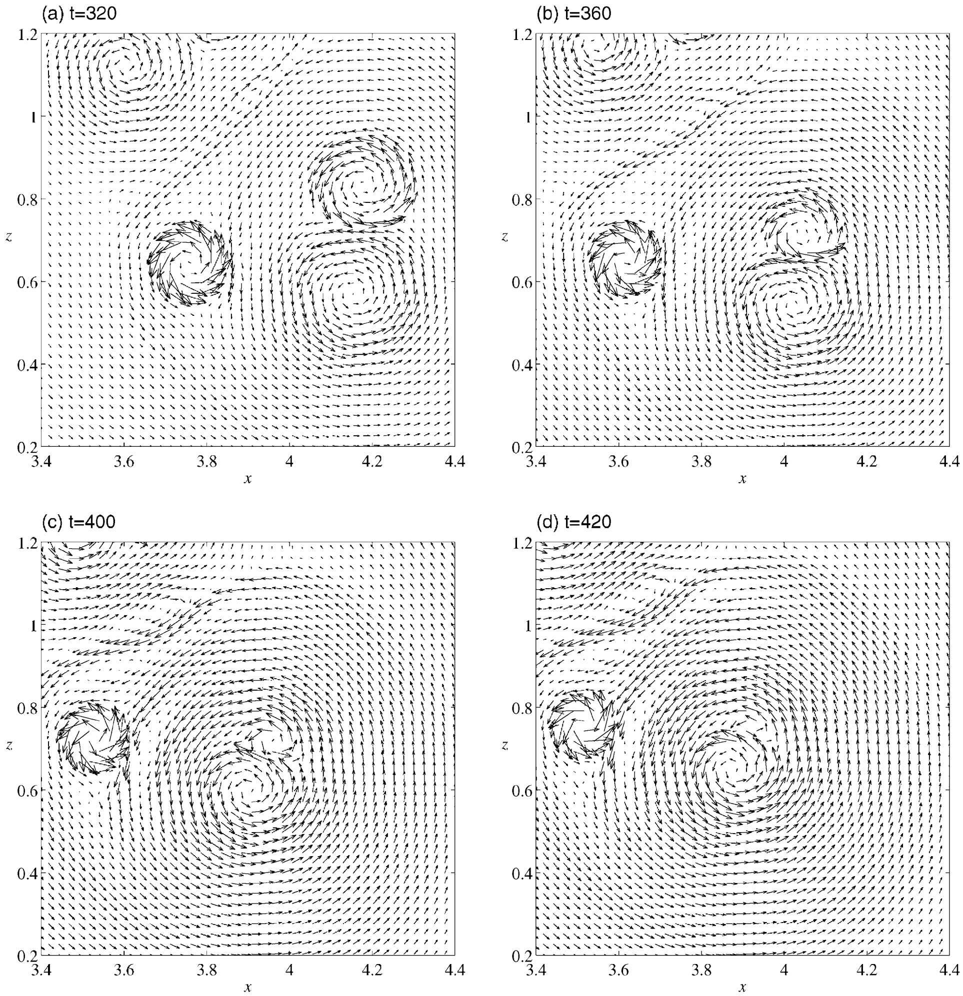


Fig. 3. Results of Case 1: merging of two magnetic islands.

magnetic field configuration on the turbulent dynamics near the magnetotail neutral sheet. In runs 2 and 3, we include a shear magnetic field to mimic the region near the magnetotail neutral sheet. The shear magnetic field is given by $B_x = 0.1\cos z$. Fig. 4 shows the results at $t = 70$, 300 and 600 of run 2. The influence of the sheared magnetic field is obvious. The coherent structures are now centered along the neutral sheets at $z \sim \pi/2$ and $3\pi/2$ with the current filaments orienting in the background current directions, which are in the $-y$ direction at $z \sim \pi/2$ and in the $+y$ direction at $z \sim 3\pi/2$. This is consistent with that proposal by Chang. Away from the neutral sheets, the fluctuating magnetic fields produce fluctuating current sheets.

The development of the coherent structure with a background shear magnetic field strongly depends on the strength of the shear field and the level of the fluctuation. The small number of magnetic islands shown in the figure indicates that the strength of the shear is strong in relation to the fluctuation. A weak shear field will evolve the same way as in the first example, where no shear is imposed, involving many coherent structures. As the strength of the shear (the intensity of background current sheet) is increased, the current sheet tends to attract the fluctuating current filaments of the same polarity to the neutral sheet, giving the results in Fig. 4. On the other hand, if there were no fluctuations or fluctuations with very small amplitudes, the sheared magnetic field configuration can at most be subject to the tearing instability. The tearing instability is rather unimportant in this case because of very small numerical diffusion terms (with respect to the scale length of the magnetic shear) in the code; no noticeable distortion of the field should be present at the time shown in Fig. 4. The shear-induced instability in the presence of existing fluctuations, as is shown in this run, is certainly a fluctuation-induced, nonlinear instability. Fig. 5 shows the effects of the initial spectra. It gives the results of run 3 at $t = 300$ and 600. The initial conditions of

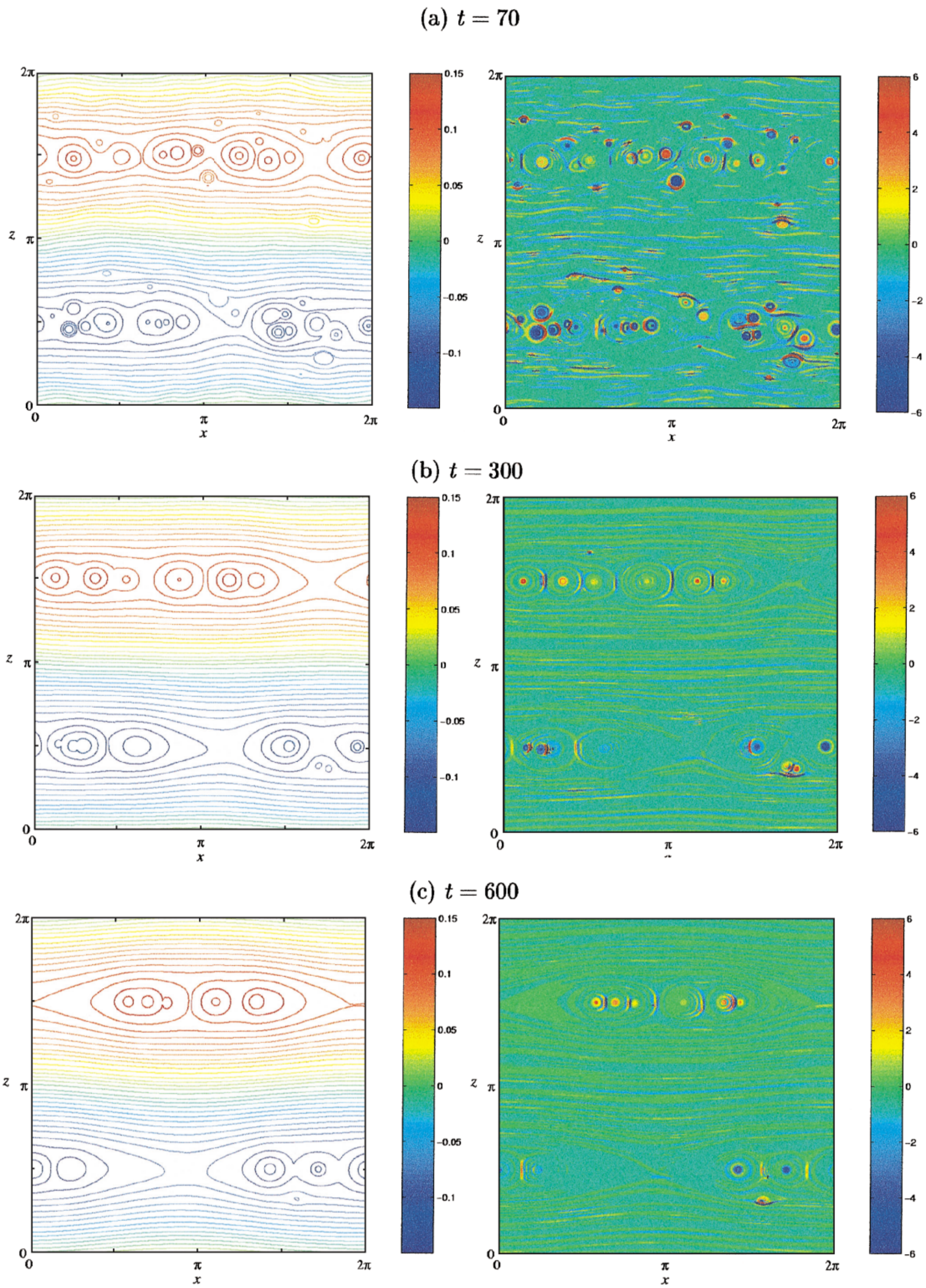


Fig. 4. Results of Case 2 at $t = 70$, 300 and 600. The magnetic field lines (contours of the magnetic flux) are shown in the left-hand side column; the corresponding current distributions $J_y$ are shown in the right-hand side column. They show the effects of magnetic shear and the resulting fluctuation-induced, nonlinear instability.

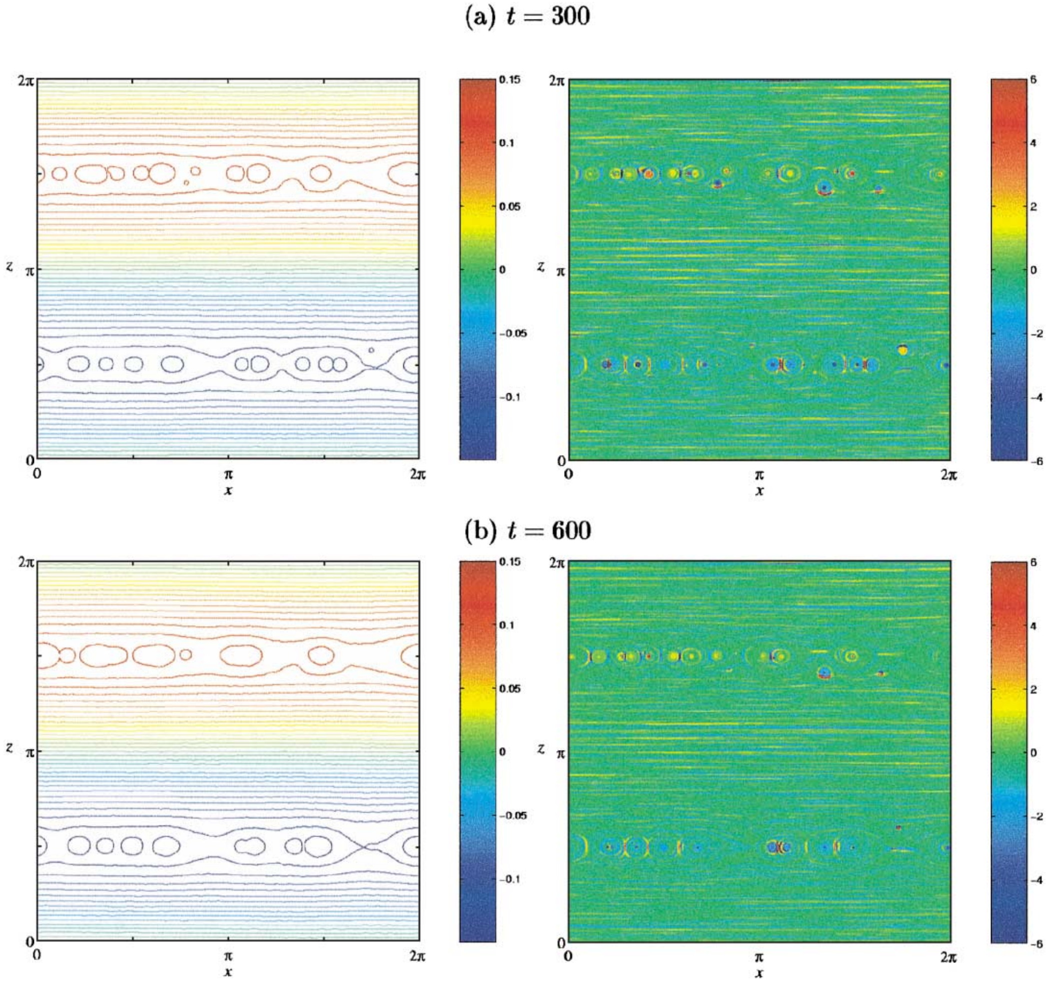


Fig. 5. Results of Case 3 at $t = 300$ and 600. The magnetic field lines (contours of the magnetic flux) are shown in the left-hand side column; the corresponding current distributions $J_y$ are shown in the right-hand side column. Case 3 has a higher initial mode number than case 2 has.

runs 2 and 3 are similar, except that the initial fluctuation is peaked at the Fourier mode $k \sim 20$ for run 3 and $k \sim 10$ for run 2. More magnetic islands are formed near the neutral sheets in run 3 than in run 2.

## 5. Conclusion

Results from new large-scale MHD simulations reconfirm our earlier preliminary calculations (Wu and Chang, 2000). The coherent structures that emerge from the simulations are force-free and circularly symmetric. The structures can merge locally and sporadically; a process that may sometimes be related to the observations of bursty bulk flows in the Earth's magnetotail when wave–particle interactions are properly considered (Angelopoulos et al., 1996, 1999). The fluctuation spectra show the long-range behavior of the stochastic system. With a sheared magnetic field to model the magnetotail neutral sheet, the coherent structures tend to align with the background current sheet and a fluctuation-induced, nonlinear instability is observed. These features are consistent with Chang's intermittent turbulence model for the magnetotail. The results also indicate that the evolution of the system can be strongly influenced by the magnetic shear and the level of fluctuation. Higher shear and larger fluctuation result in a more active system. For the magnetotail, this suggests that the system is more active under the condition of southward interplanetary magnetic field, which produces larger magnetic shear and more fluctuation in the magnetotail. This conclusion seems to agree with observations.

Our calculations are only a beginning. Future study will extend the computation from 2D to 3D so that multiple Alfvén resonances can easily be simulated. We shall also increase the numerical resolution such that small-scale turbulence through stretching, folding and tearing instability of the current sheets may occur. Ultimately, we shall carry out calculations with more realistic magnetotail configurations.

## Acknowledgements

We are grateful to Dr. Z.S. She for his interest in this study. Computing was supported by Texas Supercomputer Center through NPACI, which is sponsored by NSF. The work of CCW is supported by a NASA grant and the work of TSC is partially supported by grants from AFOSR, NSF and NASA.

## References

Angelopoulos, V., Coroniti, F.V., Kennel, C.F., Kivelson, M.G., Walker, R.J., Russell, C.T., McPherron, R.L., Sanchez, E., Meng, C.I., Baumjohann, W., Reeves, G.D., Belian, R.D., Sato, N., Fris-Christensen, E., Sutcliffe, P.R., Yumoto, K., Harris, T., 1996. Multipoint analysis of a bursty bulk flow event on April 11, 1985. Journal of Geophysical Research 101 (A3), 4967–4989.

Angelopoulos, V., Mukai, T., Kokubun, S., 1999. Evidence for intermittency in Earth's plasma sheet and implications for self-organized criticality. Physics of Plasmas 6 (11), 4161–4168.

Baker, D., Klimas, A., McPherron, R.L., Büchner, J., 1990. The evolution from weak to strong geomagnetic activity: an interpretation in terms of deterministic chaos. Geophysical Research Letters 17 (1), 41–44.

Biskamp, D., Welter, H., 1989. Dynamics of decaying two-dimensional magnetohydrodynamic turbulence. Physics of Fluids B (Plasma Physics) 1 (10), 1964–1979.

Chang, T., 1998a. Sporadic localized reconnections and multiscale intermittent turbulence in the magnetotail. In: Horwitz, J.L., Gallagher, D.L., Peterson, W.K. (Eds.), Geospace Mass and Energy Flow. Geophysical Monograph No. 104, American Geophysical Union, Washington, DC.

Chang, T., 1998b. Multiscale intermittent turbulence in the magnetotail. In: Kokubun, S., Kamide, Y. (Eds.), Proceedings of the Fourth International Conference on Substorms. Terra Scientific Publishing Company. Kluwer Academic Publishers, Dordrecht.

Chang, T., 1999. Self-organized criticality, multi-fractal spectra, sporadic localized reconnections and intermittent turbulence in the magnetotail. Physics of Plasmas 6 (11), 4137–4145.

Craddock, G.G., Diamond, P.H., Terry, P.W., 1991. The observation of isolated long-lived current filaments in two-dimensional microtearing turbulence. Physics of Fluids B (Plasma Physics) 3 (2), 304–315.

Galtier, S., Zienicke, E., Politano, H., Pouquet, A., 1999. Parametric investigation of self-similar decay laws in MHD turbulent flows. Journal of Plasma Physics 61 (3), 507–541.

Hoshino, M., Nishida, A., Yamamoto, T., Kokubum, S., 1994. Turbulence magnetic field in the distant magnetotail: bottom-up process of plasmoid formation? Geophysical Research Letter 21 (25), 2935–2938.

Kurganov, A., Tadmor, E., 1999. New high-resolution central schemes for nonlinear conservation laws and convection–diffusion equations. CAM Report 99-16, UCLA.

Klimas, A.J., Baker, D.N., Roberts, D.A., Fairfield, D.H., Büchner, J., 1992. A nonlinear dynamical analogue model of geomagnetic activity. Journal of Geophysical Research 97 (A8), 12,253–12,266.

Lui, A.T.Y., 1998. Multiscale and intermittent nature of current disruption in the magnetotail. In: Chang, T., Jasperse, J.R. (Eds.), Physics of Space Plasmas. MIT Geo/Cosmo Plasma Physics, Cambridge, MA.

Milovanov, A., Zelenyi, L., Zimbardo, G., 1996. Fractal structures and power law spectra in the distant Earth's magnetotail. Journal of Geophysical Research 101 (A9), 19903–19910.

Nessyahu, H., Tadmor, E., 1990. Non-oscillatory central differencing for hyperbolic conservation laws. Journal of Computational Physics 87 (2), 408–463.

Pritchett, P.L., Wu, C.C., 1979. Coalescence of Magnetic Islands. Physics of Fluids 22 (11), 2140–2146.

Sharma, A.S., Vassiliadis, D., Papadopoulos, K., 1993. Reconstruction of low-dimensional magnetospheric dynamics by singular spectrum analysis. Geophysical Research Letters 20 (5), 335–338.

Sergeev, V.A., Mitchell, D.G., Russell, C.T., Williams, D.J., 1993. Structure of the tail plasma/current sheet at $\sim 11R_E$ and its changes in the course of a substorm. Journal of Geophysical Research 98 (A10), 17,345.

Vassiliadis, D.V., Sharma, A.S., Eastman, T.E., Papadopoulos, K., 1990. Low-dimensional chaos in magnetospheric activity from AE time series. Geophysical Research Letters 17 (11), 1841–1844.

Wu, C.C., Chang, T.S., 2000. 2D MHD simulation of the emergence and merging of coherent structures. Geophysical Research Letters 27 (6), 863–866.